Bulletin of the Seismological Society of America, Vol. 100, No. 4, pp. 1823–1829, August 2010, doi: 10.1785/0120090152

Short Note

Ground-Motion Difference between Two Moderate-Size Intraplate Earthquakes in the United Kingdom

by L. Ottemöller and S. Sargeant

Abstract Two moderate-size earthquakes occurred in the United Kingdom, the first near Folkestone in 2007 with M_w 4.0 and the second near Market Rasen in 2008 with M_w 4.5. Both were strongly felt and caused some nonstructural damage. The earthquakes occurred at significantly different depths, the Folkestone earthquake at 5 km and the Market Rasen earthquake at 20 km. We determined the seismic moment and the stress drop of the two mainshocks, and two smaller earthquakes in the same locations, by modeling the source displacement spectra. We found stress drops of 30 ± 34 bar and 344 ± 136 bar for the Folkestone and Market Rasen mainshocks, respectively. This is a significant difference considering the earthquakes are only 275 km apart and both are of intraplate origin. We applied the stochastic ground-motion modeling technique and used the stress drop and seismic moment to compute vertical component peak ground acceleration. The modeled ground motions are consistent with the observations. We also computed vertical peak ground acceleration for a hypothetical M_w 6.0 high stress-drop (200 bar) earthquake and found that it would be 4.6 m/sec^2 at 20 km hypocentral distance.

Introduction

Two moderate-size damaging earthquakes occurred in the United Kingdom, an area of low intraplate seismicity, within a year. First, an earthquake near Folkestone on the southeast coast of Kent occurred on 28 April 2007 with a local magnitude M_L 4.3. A detailed analysis of the earthquake is given by Ottemöller and Baptie *et al.* (2009); the details of damage and felt effects are given by Sargeant *et al.* (2008). The earthquake was shallow with a depth of 5 km. Second, on 27 February 2008 an earthquake of M_L 5.2 occurred near Market Rasen, Lincolnshire, about 275 km northwest of Folkestone (Ottemöller and Sargeant *et al.*, 2009). This earthquake had a source depth of 20 km. It was felt throughout most of England and Wales in contrast to the Folkestone earthquake, which was felt in southeastern England only. This difference is explained by the Market Rasen earthquake being both larger and deeper. Following both earthquakes a number of aftershocks were recorded. A total of nine aftershocks were recorded from the Folkestone earthquake over a period of eight days; the largest was M_L 1.7. The aftershocks could not be located precisely because they were mostly recorded on only one station. Another earthquake with M_L 3.0 occurred on 3 March 2009 near the Folkestone earthquakes of 2007. We include the analysis of this event due to its location and size. The total of recorded aftershocks from the Market Rasen earthquake was also nine. The largest of these occurred on 5 April 2007 and had a magnitude M_L 2.8. The aftershocks lasted for a period of 38 days. The Market Rasen aftershocks were collocated with the mainshock within the location uncertainties. The locations and fault plane solutions of the two mainshocks are shown in Figure 1. The source mechanisms were determined through regional moment tensor inversion (Ottemöller and Sargeant *et al.*, 2009). The direction of maximum compression indicated by the fault plane solution in both cases is consistent with northwest-southeast compression from the Mid-Atlantic Ridge. However, the mechanism for the Folkestone earthquake is oblique-normal, while it is oblique-reverse for the Market Rasen earthquake.

Our aim in this article is to compare the two mainshocks in terms of their stress drop and the observed ground motion. We determine the seismic moment and stress drop from the observed vertical component S-wave displacement spectra. These parameters are then used to model the vertical acceleration using the stochastic method (Boore, 1983, 2003). We compare the modeled results with the observed ground motion. We then estimate ground motion from M_w 6.0 earthquakes for low and high stress-drop scenarios.

Source Parameters

We used data from broadband and short period stations in the United Kingdom, Belgium, and the Netherlands.

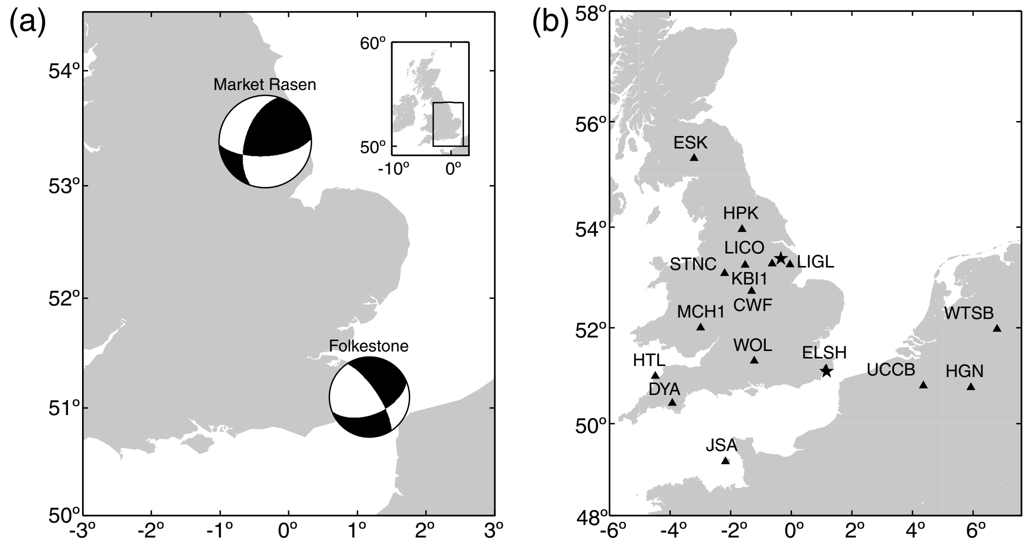

Figure 1. (a) Map showing the locations and fault plane solutions of the two mainshocks, and (b) stations shown as triangles used for spectral modeling of the two earthquakes indicated by stars.

The hypocentral distance range for our observations is 5–250 km for the Folkestone earthquakes. For the Market Rasen mainshock we use observations between 95 and 250 km, while for the largest aftershock the closest observations are at 20 km. The station locations are shown in Figure 1. The stations are founded on both bedrock and softer geology.

The observed displacement spectrum after correcting for instrumentation is given by

$$A(f) = G \times M_0 \times 2.0 \times 0.6 \times S(f) \times D(f), \quad (1)$$

where G describes geometrical spreading. Following Herrmann and Kijko (1983), we assume

$$G(R) = \begin{cases} R^{-1} & \text{for } R \leq 100 \text{ km} \\ (100 \times R)^{-1/2} & \text{for } R \geq 100 \text{ km} \end{cases} \quad (2)$$

for shear waves (S and Lg), where R (km) is the hypocentral distance. The factors 2.0 and 0.6 (equations 1 and 3) account for the effects of the free surface and radiation pattern, respectively. M_0 (Nm) is the seismic moment, which is given by

$$M_0 = 4 \times \pi \times \rho \times v_s^3 \times A_0/(G(R) \times 2.0 \times 0.6), \quad (3)$$

where we use the density $\rho = 2.7$ (g/cm^3) and the S-wave velocity at the source $v_s = 3.5$ (km/sec), and A_0 is the amplitude of the flat part of the spectrum $A(f)$ (nm sec). The earthquake source spectrum $S(f)$ is often approximated by the ω^2 model (Aki, 1967; Brune, 1970). The shape of the ω^2 source model is determined by the corner frequency f_c (Hz) by

$$S(f) \propto \frac{1}{(f/f_c)^2 + 1}. \quad (4)$$

The correction for attenuation $D(f)$ is commonly constructed in two parts. The first part accounts for attenuation along the path described by $Q(f)$ and the second accounts for near-surface attenuation κ (sec) near the receiver (Singh *et al.*, 1982)

$$D(f) = \exp\left[\frac{-\pi T f}{Q(f)}\right] \exp(-\pi \kappa f), \quad (5)$$

where T (sec) is the travel time. We used the United Kingdom average attenuation model derived for Lg waves of Sargeant and Ottemöller (2009)

$$Q(f) = 266 f^{0.53}. \quad (6)$$

This attenuation model was derived assuming the same geometrical spreading as used here (equation 2).

As the observed spectrum is the product of source and attenuation, we are dealing with a nonunique model. Assuming that the $Q(f)$ model is correct, Figure 2 illustrates the trade-off between κ and f_c for the largest Market Rasen aftershock. The figure shows the computed spectra for three different combinations of these parameters. All three are reasonable approximations of the observed spectrum, and it is clear that knowledge of κ is essential for a realistic estimate of f_c.

The near-surface attenuation can be determined from records at short hypocentral distance, where path attenuation is not significant. For frequencies below the corner frequency, κ can be determined from the slope of the displacement spectrum, which when corrected for attenuation is expected to be flat if we ignore the frequency dependency of site amplification. We determine κ from vertical component data that are less affected by site amplification. This analysis was done for Folkestone aftershocks giving $\kappa = 0.02$ sec (Ottemöller and Baptie *et al.*, 2009). We applied the same technique to the Market Rasen aftershocks below M_L 1.5 and obtained the same $\kappa = 0.02$ sec.

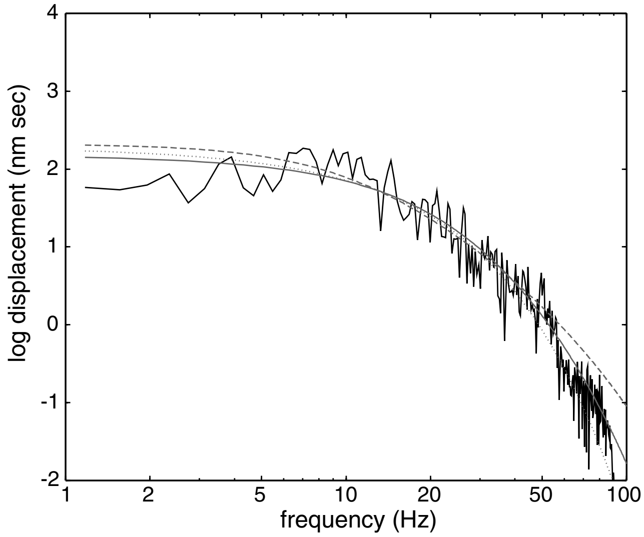

Figure 2. *Lg*-wave displacement spectrum (black) at station LICO from the Market Rasen aftershock on 5 April 2008 13:57:26 with M_L 2.8. The observed spectrum is corrected for geometrical spreading and $Q(f)$, but not κ. For comparison modeled spectra are shown in gray, dashed: $f_c = 10$ Hz and $\kappa = 0.01$ sec, solid: $f_c = 25$ Hz and $\kappa = 0.02$ sec, and dotted: $f_c = 50$ Hz and $\kappa = 0.03$ sec.

We used this κ value and $Q(f)$ as given in equation (6) to estimate the seismic moment and corner frequency for the two mainshocks, the largest Market Rasen aftershock, and the 2009 Folkestone earthquake. The spectral fitting is done using the method of Ottemöller and Havskov (2003), where M_0 and f_c are determined in a grid search. In this analysis we used vertical component data, which means that correction for site amplification is not required. We notice that $\kappa = 0.02$ sec is not appropriate for all stations, but find that the average results do not change significantly when including κ in the grid search. The observed and modeled spectra are shown in Figure 3.

From the corner frequency f_c we compute the source radius r (km) (Brune, 1970)

$$r = 0.37 v_s / f_c. \quad (7)$$

The stress-drop $\Delta\sigma$ (bar) is given by

$$\Delta\sigma = 0.44 M_0 / r^3, \quad (8)$$

assuming a circular fault (Eshelby, 1957). Uncertainties in the stress-drop determination are large as it scales as f_c^3, which itself has large uncertainties.

The results from this analysis are given in Table 1. The two Market Rasen earthquakes are characterized by relatively high stress drops (between 250 and 350 bar), whereas the stress drop for the Folkestone earthquakes is significantly lower (around 30 to 90 bar). Given that we have applied the same data processing and despite the uncertainties in determining f_c, we assume that this difference is real. However, as seen from equation (7), the source radius scales linearly with v_s. The value of $v_s = 3.5$ km/sec corresponds to the hypocentral depth of the Market Rasen earthquake. If we assume $v_s = 3$ km/sec, which is more appropriate for the depth of the Folkestone earthquake, the source radius is slightly reduced from 0.60 to 0.54 km, and the stress drop increases correspondingly from 30 to 48 bar. While it is more correct to use a depth dependent v_s, this is not commonly done in practice, so our comparison is based on the same $v_s = 3.5$ km/sec. This does not alter our main observation, that is, the Market Rasen earthquakes are associated with significantly higher stress drops than the Folkestone events.

Ground Motion

In intraplate areas with low seismicity such as the United Kingdom, there is a lack of strong motion observations. This presents a problem in seismic hazard studies, which tend to rely on ground-motion relations based on empirical data. One way to overcome this is to simulate ground motion using stochastic modeling based on the source parameters of smaller earthquakes (e.g., Toro and McGuire, 1987; Atkinson and Boore, 1995, 2006). This approach also has limitations because source parameters of larger earthquakes can differ systematically from those of smaller earthquakes.

Here we compare ground-motion observations from the earthquakes analyzed in the previous section to the ground motion modeled using the stochastic approach (Boore, 1983, 2003). The stochastic modeling is based on the source spectral shape and the attenuation model (including $\kappa = 0.02$ sec) described in the previous section, and the earthquake parameters (moment magnitude and stress drop) derived using these (Table 1). We use the SMSIM software of Boore (2005). In the stochastic modeling, a white noise time domain signal is generated with zero mean and an average unit spectral amplitude (Boore, 1983). After transformation into the frequency domain, the signal is shaped by multiplying with the frequency dependent source function. The modeling result is computed as the average from a number of runs (we use 50). Peak ground acceleration is measured after transformation to the time domain.

Our source parameters were determined from vertical component data because they are less affected by site amplification. For the two mainshocks, we find that the horizontal spectra are similar to the vertical for long periods at which the displacement spectrum is flat (Fig. 4), but there is a frequency dependent difference for higher frequencies (>4 Hz), which we assume is due to site amplification. On average, this results in larger acceleration levels on the horizontal components. This is commonly observed; for example, Toro and McGuire (1987) report values from eastern North America for the horizontal to vertical component ratio of greater than 1 with frequency dependent differences between rock and soil sites. Also, Siddiqqi and Atkinson (2002) found from the horizontal to vertical spectral ratios at rock sites in Canada site amplification increasing from 1 at 0.5 Hz to 1.2–1.6 at

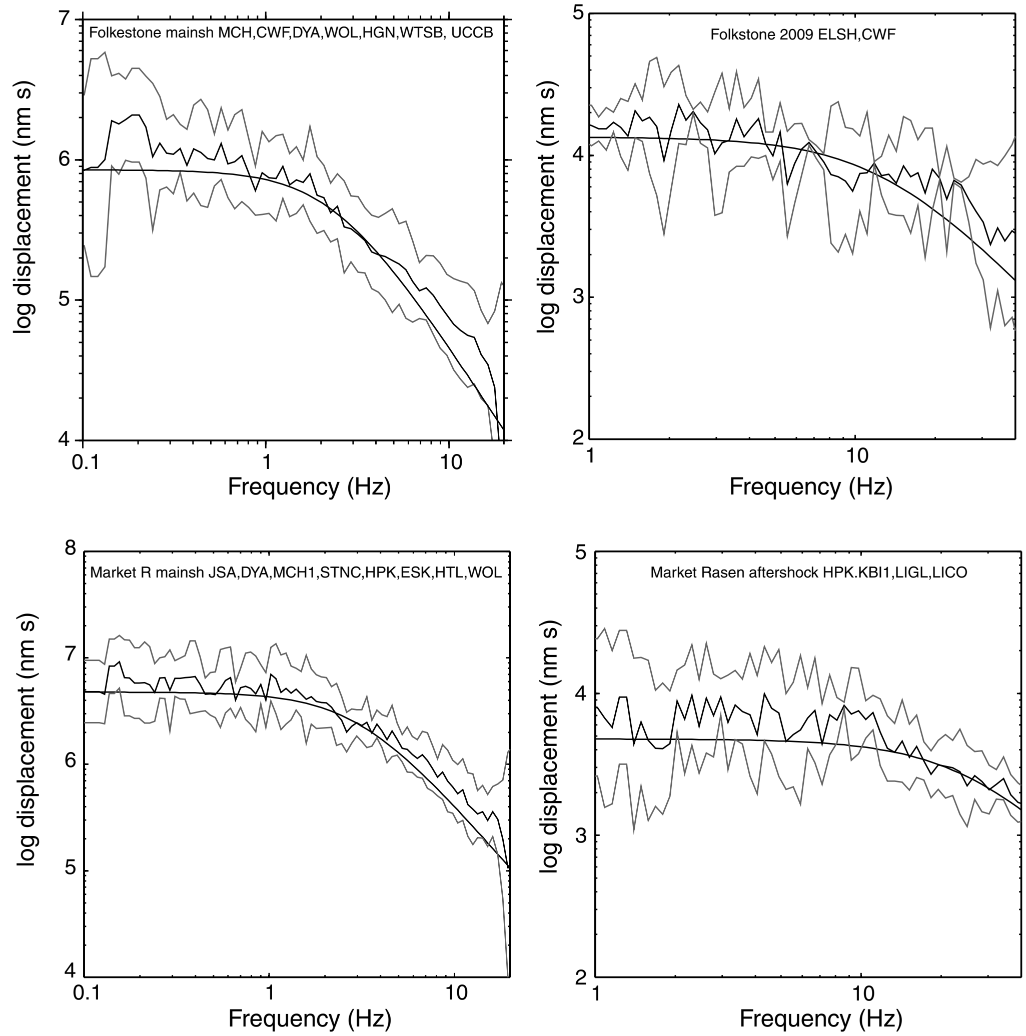

Figure 3. *Lg*-wave displacement spectra averaged from a number of stations (given in the figure) for the Folkestone mainshock and 2009 event, and Market Rasen mainshock and aftershock, corrected for geometrical spreading and attenuation (including κ). The observed smoothed spectra, plus and minus one standard deviation, are plotted in gray; the respective modeled spectra are plotted in black. The locations of the stations used are shown in Figure 1.

10 Hz. Because the site amplification is unknown for the stations used here, we restrict our ground-motion modeling to the vertical component.

In Figure 5 the results from the stochastic modeling are compared to the observed vertical accelerations (horizontal data are also shown) from the four earthquakes analyzed in the previous section. Overall, the predicted data are close to the observed peak vertical ground acceleration. The individual differences between observed and modeled vertical acceleration at each station probably results from path effects that are not accounted for in the modeling. Also, we do not account for the difference in κ between the stations. While our models for geometric spreading and the source seem to be appropriate, a reduction in the difference between the observations and modeled data may be achieved by refining these.

Table 1
Results from Spectral Analysis

Origin Time (dd/mm/yy hr:min)	Event	Depth (km)	κ (sec)	Number of Stations	f_c (Hz)	$\Delta\sigma$ (bar)	r (km)	M_w
28/04/2007 07:18	Folkestone mainshock	5	0.02	7	2.3 ± 1.0	30 ± 34	0.60	4.0 ± 0.1
03/03/2009 14:35	Folkestone 2009	5	0.02	2	14.1 ± 0.4	81 ± 7	0.09	2.7 ± 0.0
27/02/2008 00:56	Market Rasen mainshock	20	0.02	8	3.0 ± 0.7	344 ± 136	0.40	4.5 ± 0.1
05/04/2008 13:57	Market Rasen aftershock	20	0.02	4	26.7 ± 8.2	252 ± 100	0.05	2.5 ± 0.2

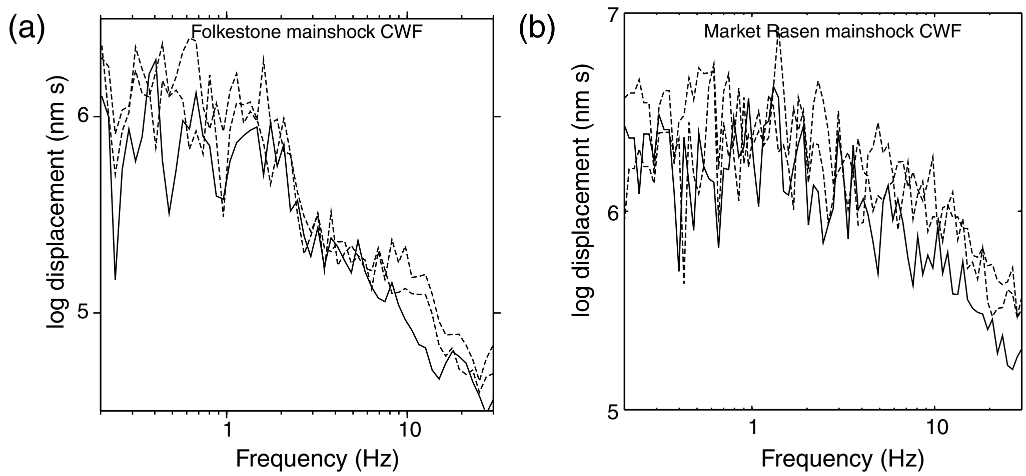

Figure 4. Comparison of vertical (solid line) and horizontal (dashed lines) component displacement spectra recorded at station CWF for the (a) Folkestone and (b) Market Rasen mainshocks.

The high stress drop of the Market Rasen earthquakes results in relatively high acceleration values for the respective seismic moments. High ground acceleration values have been observed from other high stress-drop intraplate earthquakes of moderate size, such as the M_w 4.7 Jabalpur, India, earthquake in 2000 at 27 km depth (Singh *et al.*, 2007); the M_w 4.2 Escopete, Spain, earthquake in 2008 at 6 km depth (Carreno *et al.*, 2008); and the Saguenay,

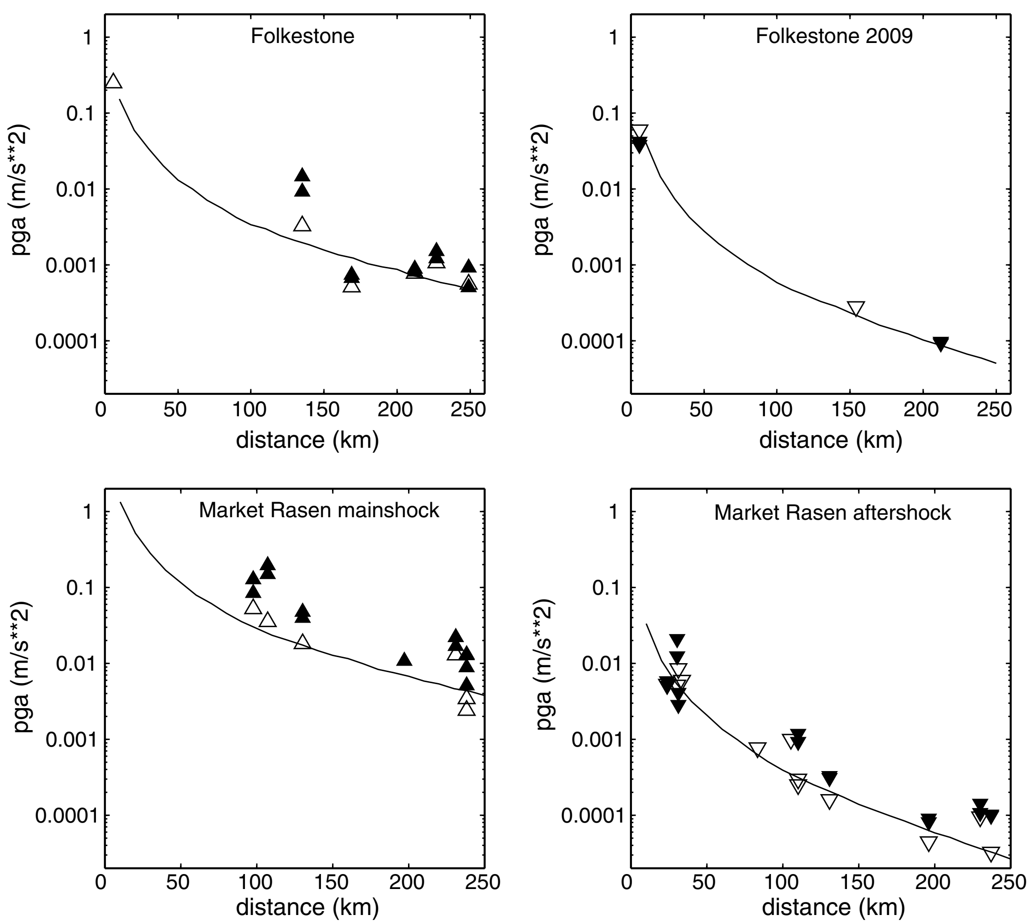

Figure 5. Ground-motion observations from the four earthquakes. Observed peak ground acceleration values are given by filled triangles for horizontal components (north–south and east–west) and by open triangles for the vertical component. The results from the stochastic modeling are based on the results given in Table 1 and $\kappa = 0.02$ sec and plotted as a black line.

Quebec, earthquake in 1988 at 28 km depth (Boore and Atkinson, 1992).

As the modeling for our events produced reasonable results, we computed peak vertical ground acceleration for a hypothetical M_w 6.0 using two stress-drop values of $\Delta\sigma =$ 20 bar and $\Delta\sigma = 200$ bar (Fig. 6) to represent low and high stress-drop scenarios. Earthquakes larger than M 6.0 are possible in the United Kingdom (Main *et al.*, 1999). The purpose of this computation is to consider the range of ground motions that might be expected for a relatively large earthquake in the U.K. and to evaluate the impact of stress drop. It is expected from equations (4), (7), and (8) that the high-frequency spectral levels scale as

$$(\Delta\sigma_1/\Delta\sigma_2)^{(2/3)}, \qquad (9)$$

so that a stress-drop increase by a factor of 10 should result in an acceleration increase by a factor of 4.6. Our results show that the computed acceleration for the higher stress-drop scenario is about five times higher (decreasing from a factor 5.6 at 50 km to a factor of 4.7 at 200 km) than for the lower stress drop. The computed acceleration for M_w 6.0 and the higher stress drop is 4.6 m/sec^2 at 20 km and 0.2 m/sec^2 at 100 km.

One may argue how realistic the modeling results are. The Market Rasen earthquake had a high stress drop, outside the range typically observed in the United Kingdom (Edwards *et al.*, 2008). It may, therefore, be considered a rare or low probability event, similar to the Saguenay earthquake (Boore and Atkinson, 1992). It has been suggested elsewhere that stress drop may increase with depth (e.g., Fletcher *et al.*, 1984; Hardebeck and Allegra, 2009). Kagawa *et al.* (2004), when looking at larger earthquakes, found higher stress drop for the deeper asperities and correlate this with higher ground motion. There are too few well-constrained data from the United Kingdom to investigate whether stress drop increases with depth. Of the high stress-drop examples given previously, only the Escopete earthquake in Spain was shallow. If the high stress-drop events were deeper, of course the hypocentral distance is greater for deeper earthquakes; the higher acceleration will be offset by the greater attenuation due to distance.

It is observed that reverse mechanisms generate higher acceleration than normal mechanisms (Boore and Atkinson, 2008). While in our case the Folkestone earthquake was oblique-normal and the Market Rasen earthquake was oblique-reverse, they both fall just outside the limit of being strike slip, according to the classification by Boore and Atkinson (2008). Overall, both the oblique-reverse mechanism and the greater depth of the Market Rasen earthquake may have contributed to the higher stress drop in accordance with observations from other places.

Conclusions

We determined the spectral source parameters from two moderate-size earthquakes in the United Kingdom and two smaller earthquakes at the respective locations. The stress drop of the Market Rasen M_w 4.5 earthquake was greater than 300 bar and about 10 times greater than the stress drop of the Folkestone M_w 4.0 earthquake. The two earthquakes were only 275 km apart, and both occurred in an area of low intraplate seismicity. The main differences between the two earthquakes are the depth of 5 km and oblique-normal mechanism for Folkestone and 20 km depth and oblique-reverse mechanism for Market Rasen.

Modeling ground acceleration using the stochastic approach based on our source parameters and a recently developed attenuation model we are able to model the vertical peak ground acceleration observations. We illustrate the effect of high stress drop that results in a relatively higher corner frequency and ground acceleration by modeling a hypothetical M_w 6.0 earthquake with stress drop of 20 and 200 bar, respectively. The ground acceleration from a high stress-drop M_w 6.0 event would be of the order of 4.6 m/sec^2 at 20 km hypocentral distance.

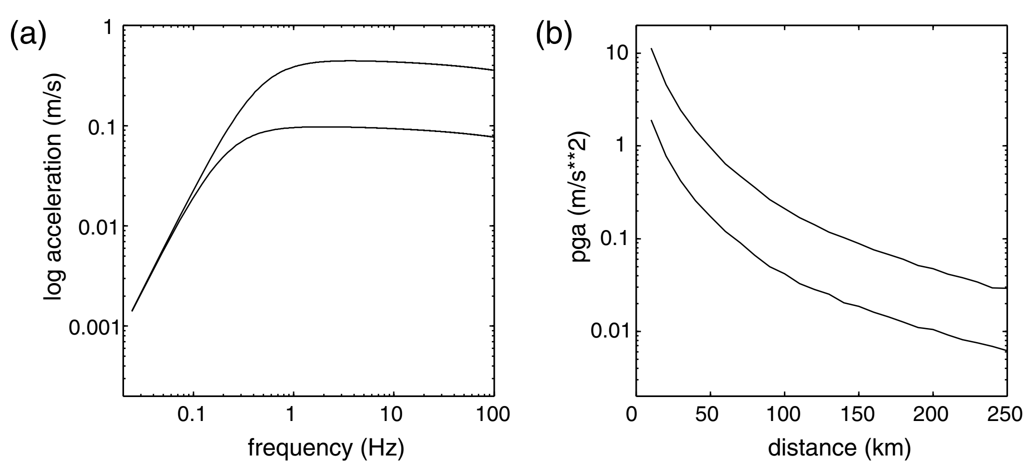

Figure 6. (a) Simulated acceleration spectra and (b) peak ground acceleration for M_w 6 and bedrock site without site amplification. The two simulations are for $\Delta\sigma = 20$ bar and $\Delta\sigma = 200$ bar, respectively. The higher value curves are for the $\Delta\sigma = 200$ bar case.

Data and Resources

Most of the data used were recorded by the seismic network operated by the British Geological Survey. We also used data recorded by the Atomic Weapons Establishment Blacknest (United Kingdom), the Royal Observatory of Belgium Seismology Section (Belgium), and The Royal Netherlands Meteorological Institute (The Netherlands). Most of the data processing was done using the SEISAN software (Havskov and Ottemöller, 2005). The SMSIM software by David Boore was used for the stochastic modeling (Boore, 2005). All our plots were created with the Generic Mapping Tools software (Wessel and Smith, 1998).

Acknowledgments

We appreciate review comments by Brian Baptie, Jens Havskov, and Roger Musson that helped to improve the manuscript. The constructive comments by two anonymous reviewers and David Boore helped to improve the manuscript significantly. This article is published with permission of the Executive Director of the British Geological Survey (NERC).

References

Aki, K. (1967). Scaling law of seismic spectrum, *J. Geophys. Res.* **72,** 1217–1231.

Atkinson, G. M., and D. M. Boore (1995). Ground-motion relations for eastern North America, *Bull. Seismol. Soc. Am.* **85,** 17–30.

Atkinson, G. M., and D. M. Boore (2006). Earthquake ground-motion prediction equations for eastern North America, *Bull. Seismol. Soc. Am.* **96,** 2181–2205.

Boore, D. M. (1983). Stochastic simulation of high-frequency ground motion based on seismological models of the radiated spectra, *Bull. Seismol. Soc. Am.* **73,** 1865–1894.

Boore, D. M. (2003). Simulation of ground motion using the stochastic method, *Pure Appl. Geophys.* **160,** 635–675.

Boore, D. M. (2005). SMSIM—Fortran programs for simulating ground motions from earthquakes: Version 2.3—A revision of OFR 96-80-A, Tech. rept., *U.S. Department of the Interior, U.S. Geological Survey*, Menlo Park, California.

Boore, D. M., and G. M. Atkinson (1992). Source spectra for the 1988 Saguneay, Quebec, earthquakes, *Bull. Seismol. Soc. Am.* **82,** 688–719.

Boore, D. M., and G. M. Atkinson (2008). Ground-motion prediction equations for the average horizontal component of PGA, PGV, and 5%-damped PSA at spectral periods between 0.01 s and 10.0 s, *Earthquake Spectra* **24,** 99–138.

Brune, J. N. (1970). Tectonic stress and the spectra of seismic shear waves from earthquakes, *J. Geophys. Res.* **75,** 4997–5009.

Carreno, E., B. Benito, J. M. M. Solares, L. Cabanas, J. Giner, P. Murphy, C. Lopez, C. del Fresno, J. M. Alcalde, J. M. Gaspar-Escribano, R. Anton, J. Martinez-Diaz, S. Cesca, A. Izquierdo, J. G. S. Cabanero, and P. Exposito (2008). The 7 June 2007 Mb *Lg* 4.2 Escopete earthquake: An event with significant ground motion in a stable zone (central Iberian Peninsula), *Seism. Res. Lett.* **79,** 820–829.

Edwards, B., A. Rietbrock, J. J. Bommer, and B. Baptie (2008). The acquisition of source, path, and site effects from microearthquake recordings using *Q* tomography: Application to the United Kingdom, *Bull. Seismol. Soc. Am.* **98,** 1915–1935.

Eshelby, J. (1957). The determination of the elastic field of an ellipsoidal inclusion and related problems, *Proc. R. Soc. London A* **241,** 376–396.

Fletcher, J., J. Boatwright, L. Haar, T. Hanks, and A. McGarr (1984). Source parameters for aftershocks of the Oroville, California, earthquake, *Bull. Seismol. Soc. Am.* **74,** 1101–1123.

Hardebeck, J. L., and A. Allegra (2009). Earthquake stress drops and inferred fault strength on the Hayward fault, East San Francisco Bay, California, *Bull. Seismol. Soc. Am.* **99,** 1801–1814.

Havskov, J., and L. Ottemöller (2005). Seisan: The earthquake analysis software for Windows, Solaris and Linux, Version 8.1. Tech. rept., Inst. of Solid Earth Physics, University of Bergen, Bergen, Norway.

Herrmann, R. B., and A. Kijko (1983). Modeling some empirical vertical component *Lg* relations, *Bull. Seismol. Soc. Am.* **73,** 157–171.

Kagawa, T., K. Irikura, and P. G. Somerville (2004). Differences in ground motion and fault rupture process between the surface and buried rupture earthquakes, *Earth Planets Space* **56,** 314.

Main, I., D. Irving, R. Musson, and A. Reading (1999). Constraints on the frequency-magnitude relation and maximum magnitudes in the UK from observed seismicity and glacio-isostatic recovery rates, *Geophys. J. Int.* **137,** 535–550.

Ottemöller, L., and J. Havskov (2003). Moment magnitude determination for local and regional earthquakes based on source spectra, *Bull. Seismol. Soc. Am.* **93,** 203–214.

Ottemöller, L., B. Baptie, and N. Smith (2009). Source Parameters for the 28 April 2007 M_W 4.0 Earthquake in Folkestone, United Kingdom, *Bull. Seismol. Soc. Am.* **99,** 1853–1867.

Ottemöller, L., S. Sargeant, and B. Baptie (2009). The M_L 5.2 Lincolnshire earthquake in 2008: A high stress drop event, in *General Assembly 2009*, European Geosciences Union, Vienna, Austria.

Sargeant, S., and L. Ottemöller (2009). *Lg* wave attenuation in Britain, *Geophys. J. Int.* **179,** no. 3, 1593–1606.

Sargeant, S. L., P. Stafford, R. Lawley, G. Weatherill, A.-J. S. Weston, J. Bommer, P. Burton, M. Free, R. M. W. Musson, A. Kuuyuor, and T. Rossetto (2008). The felt effects of the Folkestone (UK) earthquake of 28 April 2007 (4.2 M_L), *Seism. Res. Lett.* **79,** 672–687.

Siddiqqi, J., and G. M. Atkinson (2002). Ground-motion amplification at rock sites across Canada as determined from the horizontal-to-vertical component ratio, *Bull. Seismol. Soc. Am.* **92,** 877–884.

Singh, S. K., R. J. Apsel, J. Fried, and J. N. Brune (1982). Spectral attenuation of *SH* waves along the Imperial fault, *Bull. Seismol. Soc. Am.* **72,** 2003–2016.

Singh, S. K., S. Pimprikar, B. K. Bansal, J. F. Pacheco, R. S. Dattarayam, and G. Suresh (2007). An analysis of the M_w 4.7 Jabalpur, India, earthquake of 16 October 2000: Toward ground-motion estimation in the region from future events, *Bull. Seismol. Soc. Am.* **97,** 1475–1485.

Toro, G. R., and R. K. McGuire (1987). An investigation into earthquake ground motion characteristics in eastern North America, *Bull. Seismol. Soc. Am.* **77,** 468–489.

Wessel, P., and W. H. F. Smith (1998). New, improved version of the Generic Mapping Tools released, *Eos Trans. AGU* **79,** 579.

Department of Earth Science
University of Bergen
Allegt. 41,5007 Bergen, Norway
lars.ottemoller@geo.uib.no
(L.O.)

British Geological Survey
Murchison House, West Mains Road
Edinburgh, EH9 3LA, United Kingdom
(S.S.)

Manuscript received 25 June 2009